Arch. Pharm. Res. (2020) 43:1347–1355
https://doi.org/10.1007/s12272-020-01284-5

Online ISSN 1976-3786
Print ISSN 0253-6269

Archives of Pharmacal Research
www.springer.com/12272

RESEARCH ARTICLE

PBN inhibits a detrimental effect of methamphetamine on brain endothelial cells by alleviating the generation of reactive oxygen species

Jong Su Hwang[1] · Eun Hye Cha[1] · Byoungduck Park[2] · Eunyoung Ha[1] · Ji Hae Seo[1]

Received: 31 August 2020 / Accepted: 4 November 2020 / Published online: 16 November 2020
© The Pharmaceutical Society of Korea 2020

Abstract Methamphetamine (METH) is a powerful psychostimulant that is causing serious health problems worldwide owing to imprudent abuses. Recent studies have suggested that METH has deleterious effects on the blood–brain barrier (BBB). A few studies have also been conducted on the mechanisms whereby METH-induced oxidative stress causes BBB dysfunction. We investigated whether *N-tert*-butyl-α-phenylnitrone (PBN) has protective effects on BBB function against METH exposure in primary human brain microvascular endothelial cells (HBMECs). We found that METH significantly increased reactive oxygen species (ROS) generation in HBMECs. Pretreatment with PBN decreased METH-induced ROS production. With regard to BBB functional integrity, METH exposure elevated the paracellular permeability and reduced the monolayer integrity; PBN treatment reversed these effects. An analysis of the BBB structural properties, by immunostaining junction proteins and cytoskeleton in HBMECs, indicated that METH treatment changed the cellular localization of the tight (ZO-1) and adherens junctions (VE-cadherin) from the membrane to cytoplasm. Furthermore, METH induced cytoskeletal reorganization *via* the formation of robust stress fibers. METH-induced junctional protein redistribution and cytoskeletal reorganization were attenuated by PBN treatment. Our results suggest that PBN can act as a therapeutic reagent for METH-induced BBB dysfunction by inhibiting excess ROS generation.

Keywords Blood–brain barrier · Methamphetamine · *N-tert*-butyl-α-phenylnitrone · Reactive oxygen species

Introduction

Methamphetamine (METH) is one of the most addictive psychostimulants that is abused worldwide for its euphoric effects (Seo et al. 2020). The acute and chronic use of METH is associated with neuropsychiatric disorders as a consequence of neurotoxicity in the dopaminergic and serotonergic neurons in the striatum, hippocampus, and prefrontal cortex (Gold et al. 2009; Yu et al. 2015). In addition, METH-mediated neurotoxicity causes neuro-inflammation *via* the activation of microglia and astrocytes, leading to cerebrovascular dysfunction (Krasnova and Cadet 2009; Sajja et al. 2016). Several reports state that METH exposure contributes to vascular dysfunction in cardio- and cerebrovessels (Natarajan et al. 2018; Kevil et al. 2019).

The blood–brain barrier (BBB) is a critical border that maintains the homeostasis of the central nervous system between the lumen of the cerebral blood vessels and brain parenchyma. The BBB functions as a highly selective membrane barrier of endothelial cells that prevents the entry of large and potentially toxic molecules into the brain using tight junctions (TJs) as well as adherens junctions (AJs) that are connected to the cytoskeleton between adjacent cells (Ballabh et al. 2004; Daneman and Prat 2015). When the BBB integrity is compromised in disease conditions, vascular dysfunction occurs and leads to various neurodegenerative diseases (Sweeney et al. 2018). Recently, several studies have shown that METH alters

✉ Eunyoung Ha
eunyoungha@kmu.ac.kr

✉ Ji Hae Seo
seojh@kmu.ac.kr

[1] Department of Biochemistry, School of Medicine, Keimyung University, Daegu 42601, Republic of Korea

[2] College of Pharmacy, Keimyung University, Daegu 42601, Republic of Korea

the BBB functional integrity, loosening the tight connections between endothelial cells (Ramirez et al. 2009; Northrop and Yamamoto 2015). Furthermore, METH-induced BBB dysfunction was observed in the progression of numerous METH-mediated brain disorders (Bowyer and Ali 2006; Northrop and Yamamoto 2015; Sajja et al. 2016; Lappin et al. 2017).

Although most BBB molecular mechanisms following METH administration remain unclear, METH-induced generation of reactive oxygen species (ROS) has been considered one of the main effects that promote BBB breakdown. Previous studies showed that overproduction of ROS alters the phenotype of endothelial cells, causing vascular hyper-permeability, which results in brain edema and leukocyte infiltration from the blood to the brain parenchyma (Himadri et al. 2010; Di et al. 2016; Jayaraj et al. 2019). Therefore, ROS inhibition may be considered an efficient therapeutic strategy to protect BBB function against the effects of METH abuse.

N-tert-butyl-α-phenylnitrone (PBN) is a ROS scavenger; it reacts with ROS non-selectively as a potent free radical trapping reagent (Kim et al. 2010). Unlike other free radical scavengers, PBN exhibits a high level of BBB penetration (Marklund et al. 2001a). In line with this advantage, PBN has been shown to have neuroprotective effects against neuropathic pain behavior, TBI, and stroke (Cao and Phillis 1994; Zhao et al. 1994; Kim et al. 2010). Based on previous studies on revitalized brain function after treatment with PBN, we investigated whether PBN could protect the BBB from loss of integrity upon METH exposure. In this study, PBN exhibited protective effects against METH-induced oxidative stress and BBB dysfunction. Our results suggest that PBN treatment can be used as a therapeutic strategy for BBB impairment due to METH abuse.

Materials and methods

Materials and reagents

PBN (B7263) was obtained from Sigma-Aldrich (St Louis, MO, USA). Methamphetamine (METH) was obtained from the Ministry of Food and Drug Safety (Cheongju, Korea). Cell counting kit-8 (CCK-8) was purchased from Dojindo (Kumamoto, Japan). The antibodies were obtained from the following sources: ZO-1 (#40-2200), occludin (#33-1500) were from Invitrogen (Carlsbad, CA, USA), VE-cadherin (ab33168) was from Abcam (Cambridge, UK), and β-actin (sc-47778) was from Santa Cruz Biotechnology (Dallas, TX, USA).

Cell culture

Primary human brain microvascular endothelial cells (HBMECs) were purchased from Cell Systems (Kirkland, WA, USA) and cultured in endothelial growth medium containing endothelial basal medium (CC-3162, Lonza, Walkersville, MD, USA) supplemented with 2% FBS, 1% penicillin streptomycin, hEGF-B, hydrocortisone, VEGF, R3-IGF-1, ascorbic acid, hEGF, GA-1000 and heparin. HBMECs were cultured on type 1 collagen-coated tissue culture polystyrene flasks (T-flask) at 37 °C in a humidified atmosphere containing 5% CO_2.

Cell viability assay

HBMECs were seeded in 96-well plates at 2×10^4 cells per well. Cells were then treated with METH (0.1, 1.0 and 5.0 mM) and PBN (50, 500, and 5000 nM) at indicated concentrations for 24 h (Schulz et al. 1996; Qie et al. 2017). To examine the protective effect of PBN in cell viability, cells were pretreated with PBN for 2 h before METH treatment for 24 h. At the end of the treatment of METH, CCK-8 reagent was added to each well and incubated at 37 °C in a 5% CO_2 incubator for 1 h. The absorbance was measured at 452 nm using a microplate reader (Tecan, Männedorf, Switzerland) (Liu et al. 2019).

Measurement of intracellular ROS

HBMECs were plated in 96-well black polystyrene microplates were at 2×10^4 cells per well. Cells were treated with 1 mM of METH for 30 min and 60 min. To assess the scavenging ability, cells were treated with 500 nM PBN, followed by exposure to 1 mM METH for 60 min. At the end of METH treatment, cells were then incubated with 5 μM 2′,7′-dichlorofluorescin diacetate (DCF-DA) in serum-free media for 30 min at 37 °C incubator. After three washes by PBS, the intracellular ROS level was determined with the intensity of DCF-DA at multi-plate reader and captured fluorescence images under fluorescence microscopy (Axio observer A1, Carl zeiss, Overkochen, Germany) (Ramirez et al. 2009). The DCF-DA intensity was expressed as fold change vs non-treated cells.

BBB permeability assay

The transwell cell culture inserts (0.4 μm pore size, 6.5 mm diameter; Corning) were used for in vitro permeability assay. HBMECs were seeded onto the collagen-coated membrane of the inserts at a density of 4×10^4 cells per membrane. Cells were then maintained in medium at 37 °C in a humidified chamber until 100% confluency. To assess the paracellular permeability of the monolayer, FITC-dextran (70 kDa;

Sigma-Aldrich) was added into the luminal chamber at a concentration of 1 µM in 300 µl media after treatment with 1 mM METH for 24 h (Martins et al. 2013; Shi et al. 2016). After incubation of FITC-dextran for 1 h, 60 µl medium was taken from the abluminal chamber. The intensity of FITC-dextran was measured at a microplate reader (480/520 nm).

Transendothelial electrical resistance (TEER)

HBMECs were grown on the collagen-coated membrane of transwell cell culture inserts for 4 days until cells were confluent. HBMECs were treated with 500 nM PBN for 2 h, followed by 1 mM METH treatment for 24 h. Electrical resistance across the cell monolayers was measured by STX2/chopstick electrodes linked to EVOM2 (World Precision Instruments, Sarasota, USA) (Yang et al. 2017; Hwang et al. 2020). The blank value of well without cells were subtracted from all experimental TEER values to calculate the unit area resistance (Ω cm^2). The results are expressed (%) of TEER.

Western blot analysis

HBMECs were seeded in 6-well plates at a density of 2×10^5 cells per well. Cells were pre-treated with 500 nM PBN for 2 h before METH treatment for 24 h. Cells were washed by cold-PBS, lysed with radioimmunoprecipitation assay (RIPA) buffer (Thermo Fisher, Waltham, MA, USA) containing protease/phosphatase inhibitor cocktail. Protein concentration was determined by the BCA protein quantification assay, followed by equal amounts of proteins (20 µg) were loaded and separated by sodium dodecyl sulfate-polyacrylamide gel electrophoresis (SDS-PAGE; Lopez-Ramirez et al. 2012). After separation of proteins, the gels were transferred to the nitrocellulose membrane, followed by blocking with 5% skim milk in PBS-T (0.05% Tween) at room temperature for 30 min. The membranes were then incubated with the following primary antibodies overnight at 4 °C: anti-ZO-1 (1:1000; Invitrogen), anti-VE-cadherin (1:1000; Abcam), anti-occludin (1:1000; Invitrogen), and anti-β-actin (1:1000, Santa Cruz Biotechnology). The membranes were washed by PBS-T for three times and incubated with HRP-conjugated anti-rabbit secondary antibody (1:10,000; Santa Cruz Biotechnology) at room temperature for 1 h. The membranes were imaged by electro-chemiluminescence (LAS-3000).

Immunocytochemistry

HBMECs grown on collagen-coated coverslips in 24-well plates were fixed with 4% paraformaldehyde for 15 min, followed by blocking with bovine serum albumin in PBS-T (0.05% Tween) for 1 h at room temperature. Cells were then incubated overnight with the following primary antibodies: anti-ZO-1 (1:200; Invitrogen) and anti-VE-cadherin (1:300; Abcam) at 4 °C. After rinsed with PBS, cells were incubated with fluorescently-labeled anti-rabbit secondary antibodies (Alexa Fluor 488 and 568). Filamentous actin (F-actin) was labeled with phalloidin-iFluor 488 reagent (1:1000; Abcam) (Shi et al. 2016). Cells were then counterstained with 4′,6-diamidino-2-phenylindole (DAPI) for nuclear labeling. After washed by PBS, coverslips were mounted on glass slides with antifade VectaShield aqueous solution (Vector Laboratories, Burlingame, CA, USA). Fluorescence images were captured by a confocal microscope (LSM5, Carl zeiss, Overkochen, Germany). Three-dimensional (3D) plot images were generated from fluorescence images using the Interactive 3D Surface Plot plugin in Image J software and represented by height of the plot.

Statistical analysis

All data represent at least three independent experiments and are presented as the mean ± standard deviation (SD). *P* values were used for group comparisons by applying the two-tailed Student's *t*-test and less than 0.05 were considered as statistically significant.

Results

METH increases ROS generation in HBMECs

To select a non-toxic concentration of METH for subsequent experiments, we applied different METH doses (0.1, 1, and 5 mM) to HBMECs. The cell viability of HBMECs treated with different doses of METH was measured using CCK-8 (Cell Counting Kit-8) assays. Up to 1 mM of METH induced no indicative changes in the cell viability, whereas 5 mM METH significantly decreased the cell viability to approximately ~ 50% (Fig. 1a, b). Hence, we chose 1 mM of METH for the subsequent experiments. Recently, several studies have shown that METH induces overproduction of ROS, which leads to cerebrovascular dysfunction (Toborek et al. 2013). Therefore, we investigated the ROS levels in METH-exposed HBMECs using 2′,7′-dichlorofluorescin diacetate (DCF-DA). In line with the results of previous studies, METH increased ROS generation both 30 and 60 min after cell exposure (Fig. 1c, d). These data indicated that METH induced oxidative stress *via* ROS generation in HBMECs.

PBN inhibits METH-induced overproduction of ROS in HBMECs

PBN, which is a well-established free radical scavenger, exhibits neuroprotective effects against various brain disorders, such as TBI and status epilepticus (Choi et al. 2016; Kubova et al. 2018). Therefore, we determined the

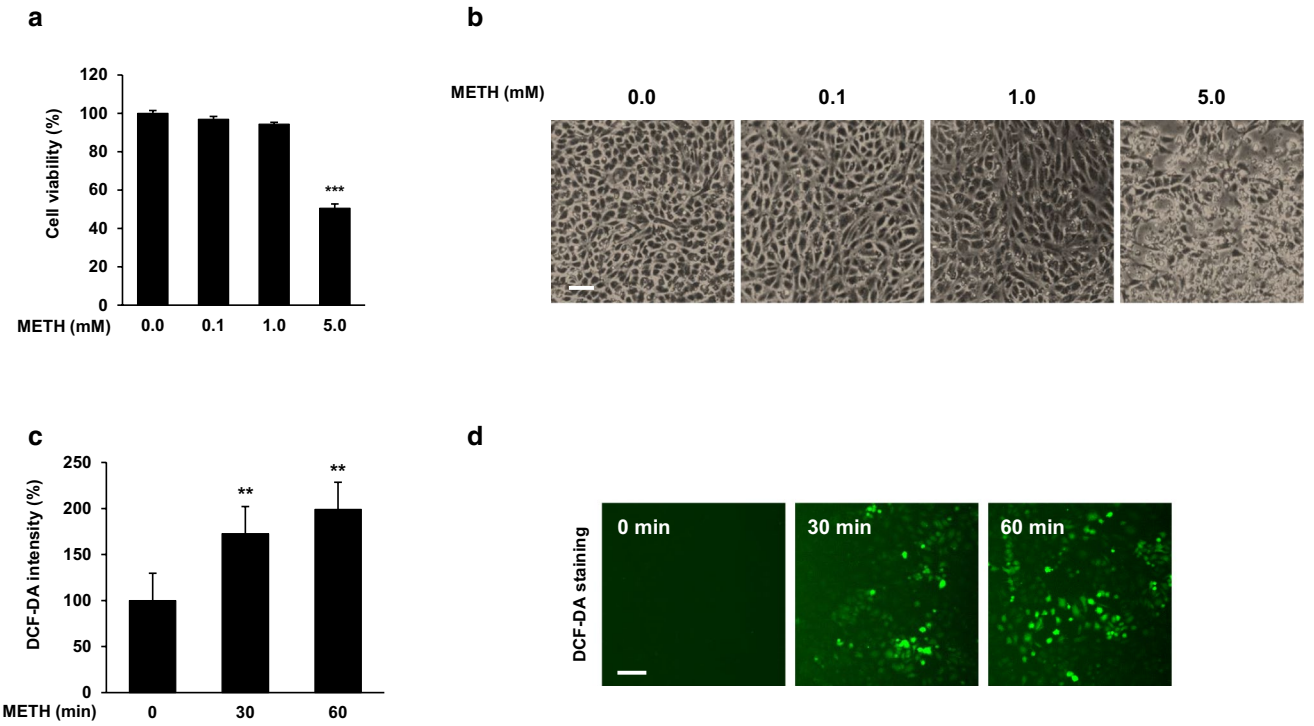

Fig. 1 METH produces excessive reactive oxygen species in HBMECs. **a** Cell viability was measured with using CCK-8 assay after treatment of METH for 24 h at indicated concentrations in HBMECs. **b** The microscopic pictures were captured after METH treatment for 24 h at indicated doses in HBMECs (scale bar 100 μm). **c** The level of intracellular ROS were detected with using 2′,7′-dichlorofluorescin diacetate after treatment of METH at 30 and 60 min in HBMECs. The fluorescence intensity of 2′,7′-dichlorofluorescin diacetate was measured at a microplate reader (485/535 nm). **d** The fluorescence images of 2′,7′-dichlorofluorescin diacetate were analyzed by a fluorescence microscope after treatment of METH for 30 min and 60 min in HBMECs (scale bar 100 μm). All data are presented as mean ± SD of three independent experiments. $^{**}p < 0.01$, $^{***}p < 0.001$

cell viability after treatment with different doses of PBN (50, 500, and 5000 nM) for 24 h. PBN concentrations up to 500 nM did not affect the cell viability, whereas 5000 nM of PBN slightly decreased the cell viability of HBMECs (Fig. 2a). Accordingly, 500 nM PBN was applied for the subsequent experiments. To investigate the inhibitory effect, HBMECs were treated with METH combined with PBN. Since previous studies used pretreatment method to determine the inhibitory effect of PBN, we pretreated HBMECs with PBN for 2 h before METH exposure (Farooque and Olsson 1997; Lee and Park 2005). As expected, PBN reduced the METH-induced ROS production in HBMECs (Fig. 2b, c). These results suggest that PBN inhibits oxidative stress resulting from METH-induced excess ROS formation.

PBN protects BBB integrity from METH-induced vascular dysfunction in HBMECs

Abnormal ROS production leads to endothelial hyperpermeability (Gilmont et al. 1998). Therefore, we investigated the protective effect of PBN on BBB function upon METH exposure. Firstly, we determined the cell viability after co-treatment with METH and PBN; there were no considerable changes in the cell viability of the HBMECs (Fig. 3a). Then, we assessed the paracellular permeability of a HBMECs monolayer using FITC-dextran, which is a fluorescent tracer for measuring barrier permeability. As shown in Fig. 3b, METH significantly increased the endothelial permeability of HBMECs; however, PBN counteracted this deleterious effect. We additionally determined the monolayer integrity of the HBMECs using the TEER assay. In accordance with previous permeability assay data, the results showed that METH reduced the monolayer integrity in HBMECs. However, this perturbation was eliminated by PBN treatment (Fig. 3c). These data suggest that PBN attenuates METH-induced BBB dysfunction.

PBN attenuates METH-induced redistribution of junction proteins in HBMECs

The BBB is composed of brain endothelial cells of the cerebral microvasculature that are tightly connected by junctional complexes consisting of TJ and AJ proteins (Jackson et al. 2019). Therefore, we firstly determined the total protein expression of junction proteins, i.e., TJ (ZO-1 and occludin) and AJ (VE-cadherin) proteins. After treatment with METH

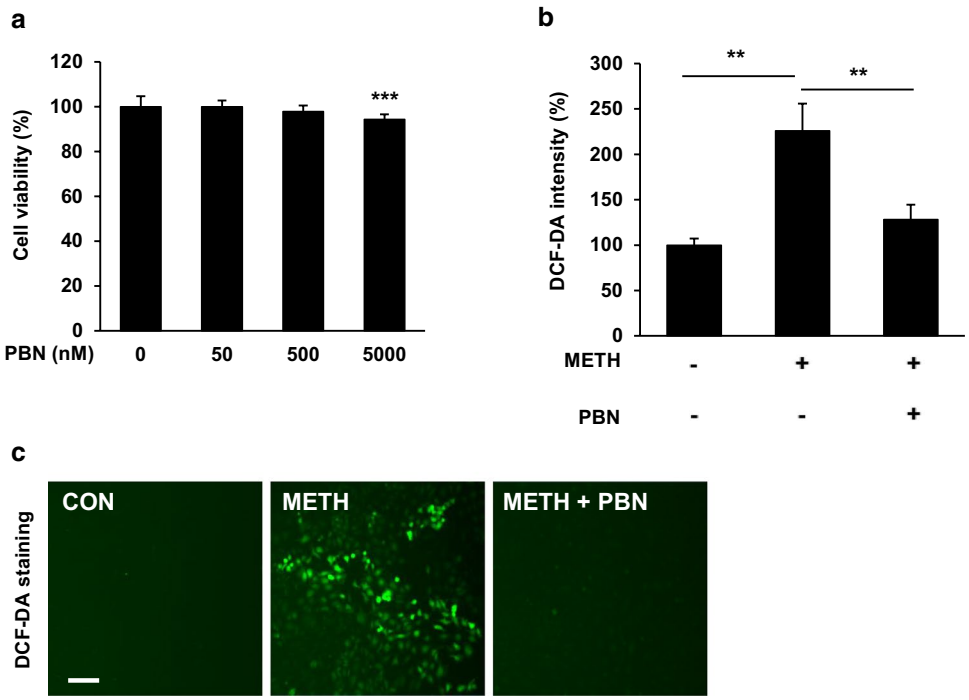

Fig. 2 METH-induced increase of ROS generation is inhibited by PBN treatment. **a** Cell viability was assessed by different doses of PBN treatment after 24 h in HBMECs. **b** The intracellular ROS levels were determined by 2′,7′-dichlorofluorescin diacetate intensity through spectrophotometry after pretreatment of 500 nM PBN for 2 h before treatment of 1 mM METH for 24 h in HBMECs. **c** The intracellular ROS were stained with 2′,7′-dichlorofluorescin diacetate and analyzed by under a fluorescence microscope after pretreatment with 500 nM PBN for 2 h, followed by treatment of 1 mM METH for 24 h in HBMECs (scale bar 100 μm). All data are presented as mean ± SD of three independent experiments. $^{**}p < 0.01$, $^{***}p < 0.001$

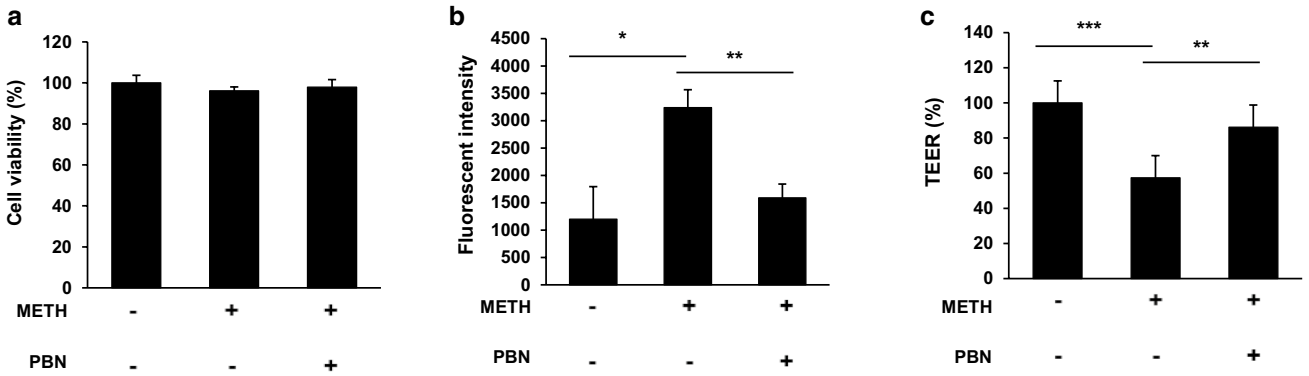

Fig. 3 PBN attenuates METH-induced vascular dysfunction in HBMECs. **a** Cell viability was evaluated with using CCK-8 reagent after pretreatment with 500 nM PBN before treatment of 1 mM METH in HBMECs. **b** Endothelial monolayer permeability was determined by fluorescence intensity of FITC-dextran (70 kDa) after treatment of 500 nM PBN and then incubated with 1 mM METH for 24 h in HBMECs. **c** Transendothelial electrical resistance values of monolayer integrity was assessed after pretreatment with 500 nM PBN for 2 h, followed by treatment of 1 mM METH for 24 h. All data are presented as mean ± SD of three independent experiments. $^{*}p < 0.05$, $^{**}p < 0.01$, $^{***}p < 0.001$

and PBN, the proteins were extracted from HBMECs and analyzed via immunoblotting. The results of western blotting revealed that the total protein expression of junction proteins was unchanged (Fig. 4a), whereas the localization of the TJ (ZO-1, red) and AJ (VE-cadherin, green) proteins partially shifted from the membrane to cytosol in METH-treated HBMECs (observed under confocal microscopy). This protein translocation was greatly reduced by PBN treatment (Fig. 4b). 3D plot images showed the height of fluorescence intensity of the junction proteins. As shown in Fig. 4c, most signals of ZO-1 and VE-cadherin in the control group were detected at cell membrane; however, these signals of junctions were translocated to the cytoplasm by METH exposure. PBN reversed the signals from the cytoplasm toward the membrane fraction. These results show that PBN reduces the redistribution of junction proteins after METH exposure.

PBN attenuates METH-induced cytoskeletal reorganization in HBMECs

Cytoskeletal rearrangement leads to morphological changes, via the formation of actin stress fibers, and

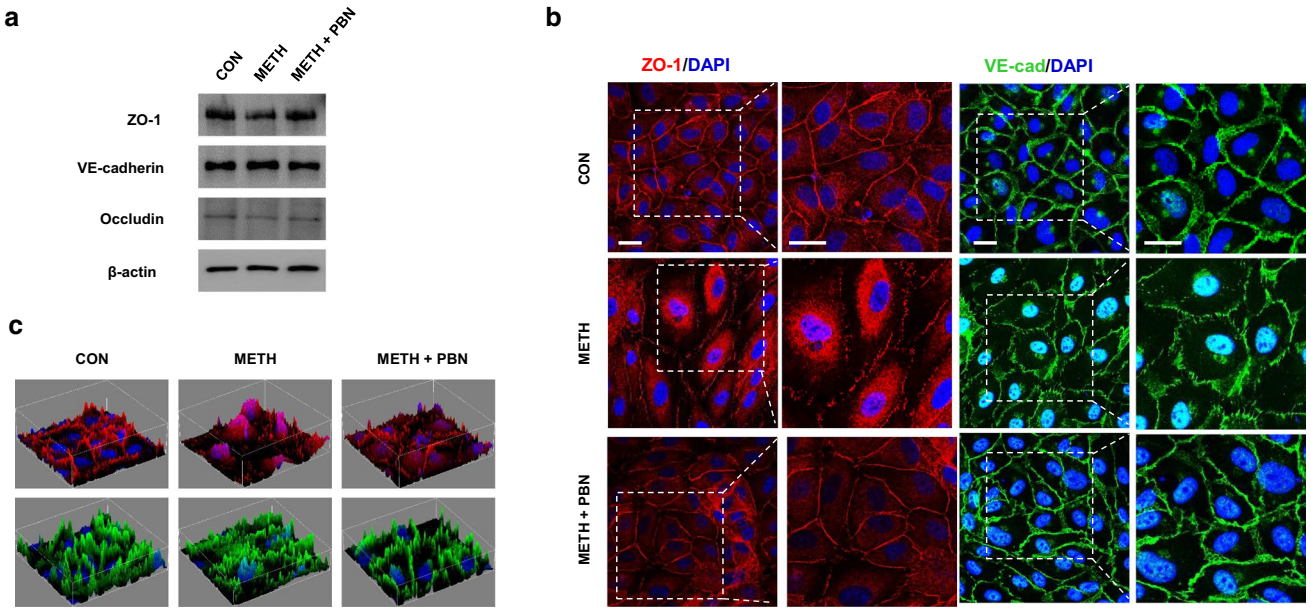

Fig. 4 PBN alleviates METH-induced localization changes of junction proteins in HBMECs. **a** Total protein expression of tight junction proteins (ZO-1 and occludin) and adhesive junction (VE-cadherin) was analyzed by western blot after treatment with 500 nM PBN for 2 h, followed by exposure of 1 mM METH for 24 h. **b** The fluorescence images of ZO-1 (red) and VE-cadherin (green) were assessed under a fluorescence microscope. Nuclei staining were performed with using 4′,6-diamidino-2-phenylindole (scale bar 20 μm). **c** Three-dimensional plot images were created from the white square dashes from **b**

induces the redistribution of junction proteins, which results in BBB dysfunction (Burridge and Wittchen 2013). After METH treatment for 24 h, we observed, under a light microscope, that METH changed the cellular morphology of HBMECs. However, PBN inhibited these morphological changes (Fig. 5a). In accordance with this phenomena, we examined whether METH could induce the formation of stress fibers in HBMECs. We found that F-actin stress fibers were strongly induced in METH-treated cells, whereas PBN prevented stress fiber formation induced by METH in HBMECs (Fig. 5b). These results indicate that

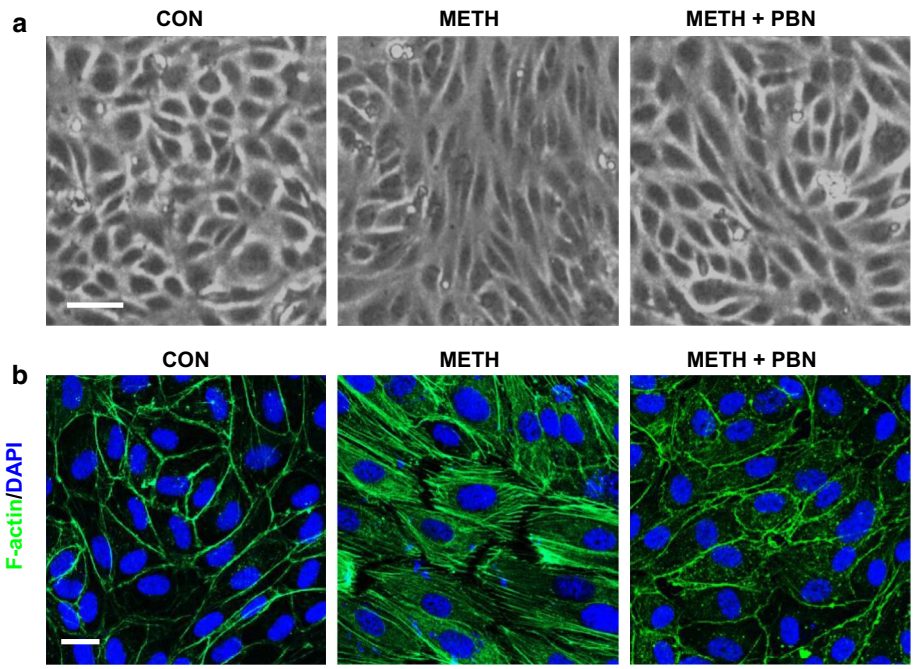

Fig. 5 PBN inhibits METH-elicited alteration of cytoskeletal structure. **a** Representative images of cellular morphology under a light microscopy after pretreatment of 500 nM PBN for 2 h before treatment of 1 mM METH for 24 h in HBMECs (scale bar 100 μm). **b** Filamentous actin was stained for fluorescein phalloidin (green) in HBMECs. Nuclei were labeled with 4′,6-diamidino-2-phenylindole (scale bar 20 μm)

PBN preserves the vascular endothelial morphology by inhibiting METH-induced cytoskeletal reorganization.

Discussion

METH is a highly addictive psychostimulant that has a strong neurotoxic effect. Although the effect of METH on dopamine neurotransmission has been well studied, METH-induced vascular toxicity and BBB dysfunction has attracted considerable attention recently as an important pathological facet of METH exposure (Sajja et al. 2016). Herein, the protective effects of PBN against METH-induced BBB impairment have been presented. PBN, a free radical scavenger, shows great efficacy in alleviating neurodegenerative diseases as well as vascular dysfunction by inhibiting ROS-induced oxidative stress (Marklund et al. 2001b; Floyd et al. 2013). ROS are well-known factors that participate in many pathological conditions (Huynh and Heo 2019; Park et al. 2019). It has been reported that induction of ROS by METH causes oxidative stress in brain tissue, leading to neuronal and vascular damage (Gold et al. 2009). Hence, we hypothesized that inhibition of METH-induced ROS accumulation via PBN treatment may have a protective effect on BBB function.

In various pathological conditions, excessive ROS have been proposed to cause BBB dysfunction by damaging the BBB structure (Pun et al. 2009). The present study revealed that METH increases the paracellular permeability and decreases the monolayer integrity of HBMECs via excessive ROS production. Previous studies have suggested that inhibition of ROS provides a neuroprotective effect under pathological conditions (Dumont and Beal 2011; Yang et al. 2019). Our results demonstrated that PBN exerts protective effects against METH-induced BBB leakage by inhibiting excessive ROS generation in HBMECs (Figs. 2, 3). These results are in accordance with those of previous studies, which showed that PBN inhibited ROS-induced oxidative stress, contributing to the maintenance of vascular function under pathological conditions (Marklund et al. 2001a).

TJs and AJs that are linked to the cytoskeleton are major components of the BBB structure. In the current study, METH disrupted TJ and AJ proteins in HBMECs. However, it did not affect the expression of endothelial junction proteins but changed their subcellular localization from the membrane to cytoplasm (Fig. 4). Previous studies have indicated that junction proteins anchored to the actin cytoskeleton are disassembled by stress fiber formation, facilitating the internalization of these proteins (Shen and Turner 2005; Vandenbroucke et al. 2008). Our results showed that METH treatment induced the generation of excessive stress fibers, resulting in phenotype alterations in HBMECs (Fig. 5). ROS decrease the BBB integrity *via* actin cytoskeletal reorganization and redistribution of junction proteins (Schreibelt et al. 2007). The mechanism involved in ROS-induced disruption of TJ and AJ includes protein modifications, such as phosphorylation, thiol oxidation, nitration, and carbonylation (Rao 2008). ROS-mediated protein modifications trigger the activation of diverse signaling molecules, including c-Src, ras homolog family member A (RhoA), protein kinase C (PKC), phosphoinositide 3-kinase (PI3K), and mitogen-activated protein kinase (MAPK), which directly or indirectly target the junction proteins, leading to the dissociation of junction protein complex and loss of their association with cytoskeleton (Blasig and Haseloff 2011). By preserving the BBB integrity after METH treatment, PBN prevented METH-induced internalization of TJ and AJ proteins by inhibiting stress fiber formation upon METH treatment (Figs. 4, 5). These observations reveal that PBN inhibits METH-induced formation of stress fibers, and thereby the redistribution of junction proteins in HBMECs.

In METH-administered animal models, inflammatory cytokines such as MMPs and TNF-α were identified as the main factors that contributed to BBB disruption (Coelho-Santos et al. 2015; Northrop and Yamamoto 2015; Namyen et al. 2020). However, METH exposure did not increase MMP-9 or TNF-α levels in HBMECs in our result (data not shown). This might imply that MMP-9 and TNF-α are vastly released from neurons, astrocytes, or microglia rather than the endothelium in METH-exposed animal models.

Although this study demonstrates the protective effect of PBN on BBB function in METH-exposed HBMECs, further studies are necessary to investigate the effect of PBN on BBB protection in METH-abuse animal models. In a clinical study, METH-dependent patients had a lower anti-oxidant capacity compared to the control group, suggesting the protective role of ROS scavengers against METH-induced brain dysfunction (Walker et al. 2014). Moreover, preclinical studies showed that PBN reduced cocaine-seeking behavior in an animal model wherein the BBB was broken after cocaine administration (Sharma et al. 2009; Jang et al. 2015). In addition, BBB dysfunction was severe in the spontaneous withdrawal stage of morphine and METH (Sharma and Ali 2006). Therefore, further studies to investigate the relationship between BBB dysfunction and withdrawal symptoms, such as depression and anxiety, or drug addiction, in abuse-animal models will be of merit (Schaefer et al. 2017).

In conclusion, this study demonstrates that PBN attenuates METH-induced BBB dysfunction in HBMECs. Our data show that METH exposure stimulates BBB dysfunction by enhancing oxidative stress. Furthermore, PBN remarkably reduces ROS generation and counteracts the harmful effects of METH on BBB function. These results suggest that PBN is a promising reagent for protecting the BBB against the effects of METH exposure.

Acknowledgements This work was supported by the Basic Science Research Program through the National Research Foundation of Korea (NRF) funded by the Ministry of Education (NRF-2016R1A6A1A03011325) and the Korean Government (MSIT) (NRF-2019R1C1C1005855, NRF-2018R1A2B6006175).

Compliance with ethical standards

Conflict of interest The authors declare no conflicts of interest.

References

Ballabh P, Braun A, Nedergaard M (2004) The blood–brain barrier: an overview: structure, regulation, and clinical implications. Neurobiol Dis 16:1–13. https://doi.org/10.1016/j.nbd.2003.12.016

Blasig IE, Haseloff RF (2011) Tight junctions and tissue barriers. Antioxid Redox Signal 15:1163–1166. https://doi.org/10.1089/ars.2011.4003

Bowyer JF, Ali S (2006) High doses of methamphetamine that cause disruption of the blood–brain barrier in limbic regions produce extensive neuronal degeneration in mouse hippocampus. Synapse 60:521–532. https://doi.org/10.1002/syn.20324

Burridge K, Wittchen ES (2013) The tension mounts: stress fibers as force-generating mechanotransducers. J Cell Biol 200:9–19. https://doi.org/10.1083/jcb.201210090

Cao XH, Phillis JW (1994) Alpha-phenyl-*tert*-butyl-nitrone reduces cortical infarct and edema in rats subjected to focal ischemia. Brain Res 644:267–272. https://doi.org/10.1016/0006-8993(94)91689-6

Choi YK, Maki T, Mandeville ET, Koh SH, Hayakawa K, Arai K, Kim YM, Whalen MJ, Xing CH, Wang XY, Kim KW, Lo EH (2016) Dual effects of carbon monoxide on pericytes and neurogenesis in traumatic brain injury. Nat Med 22:1335–1341. https://doi.org/10.1038/nm.4188

Coelho-Santos V, Leitao RA, Cardoso FL, Palmela I, Rito M, Barbosa M, Brito MA, Fontes-Ribeiro CA, Silva AP (2015) The TNF-alpha/NF-kappa B signaling pathway has a key role in methamphetamine-induced blood–brain barrier dysfunction. J Cereb Blood Flow Metab 35:1260–1271. https://doi.org/10.1038/jcbfm.2015.59

Daneman R, Prat A (2015) The blood–brain barrier. Cold Spring Harb Perspect Biol 7:a020412. https://doi.org/10.1101/cshperspect.a020412

Di A, Mehta D, Malik AB (2016) ROS-activated calcium signaling mechanisms regulating endothelial barrier function. Cell Calcium 60:163–171. https://doi.org/10.1016/j.ceca.2016.02.002

Dumont M, Beal MF (2011) Neuroprotective strategies involving ROS in Alzheimer disease. Free Radic Biol Med 51:1014–1026. https://doi.org/10.1016/j.freeradbiomed.2010.11.026

Farooque M, Olsson Y (1997) Pretreatment with alpha-phenyl-*N*-*tert*-butyl-nitrone (PBN) improves energy metabolism after spinal cord injury in rats. J Neurotrauma 14(7):469–476. https://doi.org/10.1089/neu.1997.14.469

Floyd RA, Neto HCCF, Zimmerman GA, Hensley K, Towner RA (2013) Nitrone-based therapeutics for neurodegenerative diseases: their use alone or in combination with lanthionines. Free Radic Biol Med 62:145–156. https://doi.org/10.1016/j.freeradbiomed.2013.01.033

Gilmont RR, Dardano A, Young M, Engle JS, Adamson BS, Smith DJ, Rees RS (1998) Effects of glutathione depletion on oxidant-induced endothelial cell injury. J Surg Res 80:62–68. https://doi.org/10.1006/jsre.1998.5328

Gold MS, Kobeissy FH, Wang KKW, Merlo LJ, Bruijnzeel AW, Krasnova IN, Cadet JL (2009) Methamphetamine- and trauma-induced brain injuries: comparative cellular and molecular neurobiological substrates. Biol Psychiatry 66:118–127. https://doi.org/10.1016/j.biopsych.2009.02.021

Himadri P, Kumari SS, Chitharanjan M, Dhananjay S (2010) Role of oxidative stress and inflammation in hypoxia-induced cerebral edema: a molecular approach. High Alt Med Biol 11:231–244. https://doi.org/10.1089/ham.2009.1057

Huynh DTN, Heo KS (2019) Therapeutic targets for endothelial dysfunction in vascular diseases. Arch Pharmacal Res 42:848–861. https://doi.org/10.1007/s12272-019-01180-7

Hwang JS, Cha EH, Ha EY, Park BD, Seo JH (2020) GKT136901 protects primary human brain microvascular endothelial cells against methamphetamine-induced blood–brain barrier dysfunction. Life Sci 256:117917. https://doi.org/10.1016/j.lfs.2020.117917

Jackson S, Meeks C, Vezina A, Robey RW, Tanner K, Gottesman MM (2019) Model systems for studying the blood–brain barrier: applications and challenges. Biomaterials 214:119217. https://doi.org/10.1016/j.biomaterials.2019.05.028

Jang EY, Ryu YH, Lee BH, Chang SC, Yeo MJ, Kim SH, Folsom RJ, Schilaty ND, Kim KJ, Yang CH, Steffensen SC, Kim HY (2015) Involvement of reactive oxygen species in cocaine-taking behaviors in rats. Addict Biol 20:663–675. https://doi.org/10.1111/adb.12159

Jayaraj RL, Azimullah S, Beiram R, Jalal FY, Rosenberg GA (2019) Neuroinflammation: friend and foe for ischemic stroke. J Neuroinflamm 16:142. https://doi.org/10.1186/s12974-019-1516-2

Kevil CG, Goeders NE, Woolard MD, Bhuiyan MS, Dominic P, Kolluru GK, Arnold CL, Traylor JG, Orr AW (2019) Methamphetamine use and cardiovascular disease in search of answers. Arterioscler Thromb Vasc Biol 39:1739–1746. https://doi.org/10.1161/Atvbaha.119.312461

Kim HK, Zhang YP, Gwak YS, Abdi S (2010) Phenyl *n*-*tert*-butylnitrone, a free radical scavenger, reduces mechanical allodynia in chemotherapy-induced neuropathic pain in rats. Anesthesiology 112:432–439. https://doi.org/10.1097/ALN.0b013e3181ca31bd

Krasnova IN, Cadet JL (2009) Methamphetamine toxicity and messengers of death. Brain Res Rev 60:379–407. https://doi.org/10.1016/j.brainresrev.2009.03.002

Kubova H, Folbergrova J, Rejchrtova J, Tsenov G, Parizkova M, Burchfiel J, Mikulecka A, Mares P (2018) The free radical scavenger *n*-*tert*-butyl-alpha-phenylnitrone (PBN) administered to immature rats during status epilepticus alters neurogenesis and has variable effects, both beneficial and detrimental, on long-term outcomes. Front Cell Neurosci 12:266. https://doi.org/10.3389/fncel.2018.00266

Lappin JM, Darke S, Farrell M (2017) Stroke and methamphetamine use in young adults: a review. J Neurol Neurosurg Psychiatry 88:1079–1091. https://doi.org/10.1136/jnnp-2017-316071

Lee JH, Park JW (2005) The effect of alpha-phenyl-*n*-*t*-butylnitrone on ionizing radiation-induced apoptosis in U937 cells. Free Radic Res 39:1325–1333. https://doi.org/10.1080/10715760500217215

Liu HQ, An YW, Hu AZ, Li MH, Wu JL, Liu L, Shi Y, Cui GH, Chen Y (2019) Critical roles of the PI3K-Akt-mTOR signaling pathway in apoptosis and autophagy of astrocytes induced by methamphetamine. Open Chem 17:96–104. https://doi.org/10.1515/chem-2019-0015

Lopez-Ramirez MA, Fischer R, Torres-Badillo CC, Davies HA, Logan K, Pfizenmaier K, Male DK, Sharrack B, Romero IA (2012) Role of caspases in cytokine-induced barrier breakdown in human brain endothelial cells. J Immunol 189:3130–3139. https://doi.org/10.4049/jimmunol.1103460

Marklund N, Clausen F, Lewen A, Hovda DA, Olsson Y, Hillered L (2001) Alpha-phenyl-*tert*-*n*-butyl nitrone (PBN) improves functional and morphological outcome after cortical contusion injury

in the rat. Acta Neurochir 143:73–81. https://doi.org/10.1007/s007010170141

Marklund N, Lewander T, Clausen FH, Illered L (2001) Effects of the nitrone radical scavengers PBN and S-PBN on in vivo trapping of reactive oxygen species after traumatic brain injury in rats. J Cereb Blood Flow Metab 21:1259–1267. https://doi.org/10.1097/00004647-200111000-00002

Martins T, Burgoyne T, Kenny BA, Hudson N, Futter CE, Ambrosio AF, Silva AP, Greenwood J, Turowski P (2013) Methamphetamine-induced nitric oxide promotes vesicular transport in blood–brain barrier endothelial cells. Neuropharmacology 65:74–82. https://doi.org/10.1016/j.neuropharm.2012.08.021

Namyen J, Permpoonputtana K, Nopparat C, Tocharus J, Tocharus C, Govitrapong P (2020) Protective effects of melatonin on methamphetamine-induced blood–brain barrier dysfunction in rat model. Neurotox Res 37:640–660. https://doi.org/10.1007/s12640-019-00156-1

Natarajan R, Mitchell CM, Harless N, Yamamoto BK (2018) Cerebrovascular injury after serial exposure to chronic stress and abstinence from methamphetamine self-administration. Sci Rep 8:10558. https://doi.org/10.1038/s41598-018-28970-1

Northrop NA, Yamamoto BK (2015) Methamphetamine effects on blood–brain barrier structure and function. Front Neurosci Switz 9:69. https://doi.org/10.3389/fnins.2015.00069

Park S, Kang HJ, Jeon JH, Kim MJ, Lee IK (2019) Recent advances in the pathogenesis of microvascular complications in diabetes. Arch Pharmacal Res 42:252–262. https://doi.org/10.1007/s12272-019-01130-3

Pun PBL, Lu J, Moochhala S (2009) Involvement of ROS in BBB dysfunction. Free Radic Res 43:348–364. https://doi.org/10.1080/10715760902751902

Qie XJ, Wen D, Guo HY, Xu GJ, Liu S, Shen QC, Liu Y, Zhang WF, Cong B, Ma CL (2017) Endoplasmic reticulum stress mediates methamphetamine-induced blood–brain barrier damage. Front Pharmacol 8:639. https://doi.org/10.3389/fphar.2017.00639

Ramirez SH, Potula R, Fan S, Eidem T, Papugani A, Reichenbach N, Dykstra H, Weksler BB, Romero IA, Couraud PO, Persidsky Y (2009) Methamphetamine disrupts blood–brain barrier function by induction of oxidative stress in brain endothelial cells. J Cereb Blood Flow Metab 29:1933–1945. https://doi.org/10.1038/jcbfm.2009.112

Rao R (2008) Oxidative stress-induced disruption of epithelial and endothelial tight junctions. Front Biosci 13:7210–7226. https://doi.org/10.2741/3223

Sajja RK, Rahman S, Cucullo L (2016) Drugs of abuse and blood–brain barrier endothelial dysfunction: a focus on the role of oxidative stress. J Cereb Blood Flow Metab 36:539–554. https://doi.org/10.1177/0271678x15616978

Schaefer CP, Tome ME, Davis TP (2017) The opioid epidemic: a central role for the blood brain barrier in opioid analgesia and abuse . Fluids Barriers CNS 14:32. https://doi.org/10.1186/s12987-017-0080-3

Schreibelt G, Kooij G, Reijerkerk A, van Doorn R, Gringhuis SI, van der Pol S, Weksler BB, Romero IA, Couraud PO, Piontek J, Blasig IE, Dijkstra CD, Ronken E, de Vries HE (2007) Reactive oxygen species alter brain endothelial tight junction dynamics via RhoA, PI3 kinase, and PKB signaling. FASEB J 21:3666–3676. https://doi.org/10.1096/fj.07-8329com

Schulz JB, Weller M, Klockgether T (1996) Potassium deprivation-induced apoptosis of cerebellar granule neurons: a sequential requirement for new mRNA and protein synthesis, ICE-like protease activity, and reactive oxygen species. J Neurosci 16:4696–4706. https://doi.org/10.1523/JNEUROSCI.16-15-04696.1996

Seo MJ, Song SH, Kim S, Jang WJ, Jeong CH, Lee S (2020) Characteristics of Korean patients with methamphetamine use disorder based on the quantitative analysis of methamphetamine and amphetamine in hair. Arch Pharmacal Res 43:798–807. https://doi.org/10.1007/s12272-020-01259-6

Sharma HS, Ali SF (2006) Alterations in blood–brain barrier function by morphine and methamphetamine. Ann N Y Acad Sci 1074:198–224. https://doi.org/10.1196/annals.1369.020

Sharma HS, Muresanu D, Sharma A, Patnaik R (2009) Cocaine-induced breakdown of the blood–brain barrier and neurotoxicity. Int Rev Neurobiol 88:297–334. https://doi.org/10.1016/S0074-7742(09)88011-2

Shen L, Turner JR (2005) Actin depolymerization disrupts tight junctions via caveolae-mediated endocytosis. Mol Biol Cell 16:3919–3936. https://doi.org/10.1091/mbc.E04-12-1089

Shi YJ, Zhang LL, Pu HJ, Mao LL, Hu XM, Jiang XY, Xu N, Stetler RA, Zhang F, Liu XR, Leak RK, Keep RF, Ji XM, Chen J (2016) Rapid endothelial cytoskeletal reorganization enables early blood–brain barrier disruption and long-term ischaemic reperfusion brain injury. Nat Commun 7:10523. https://doi.org/10.1038/ncomms10523

Sweeney MD, Sagare AP, Zlokovic BV (2018) Blood–brain barrier breakdown in Alzheimer disease and other neurodegenerative disorders. Nat Rev Neurol 14:133–150. https://doi.org/10.1038/nrneurol.2017.188

Toborek M, Seelbach MJ, Rashid CS, Andras IE, Chen L, Park M, Esser KA (2013) Voluntary exercise protects against methamphetamine-induced oxidative stress in brain microvasculature and disruption of the blood–brain barrier. Mol Neurodegener 8:22. https://doi.org/10.1186/1750-1326-8-22

Yang S, Mei SH, Jin H, Zhu B, Tian Y, Huo JP, Cui X, Guo AC, Zhao ZG (2017) Identification of two immortalized cell lines, ECV304 and bEnd3, for in vitro permeability studies of blood–brain barrier. PLoS ONE 12:e0187017. https://doi.org/10.1371/journal.pone.0187017

Yang QW, Huang QY, Hu ZP, Tang XQ (2019) Potential neuroprotective treatment of stroke: targeting excitotoxicity, oxidative stress, and inflammation. Front Neurosci 13:1036. https://doi.org/10.3389/fnins.2019.01036

Yu SB, Zhu L, Shen Q, Bai X, Di XH (2015) Recent advances in methamphetamine neurotoxicity mechanisms and its molecular pathophysiology. Behav Neurol 2015:103969. https://doi.org/10.1155/2015/103969

Vandenbroucke E, Mehta D, Minshall R, Malik AB (2008) Regulation of endothelial junctional permeability. Ann N Y Acad Sci 1123:134–145. https://doi.org/10.1196/annals.1420.016

Walker J, Winhusen T, Storkson JM, Lewis D, Pariza MW, Somoza E, Somoza V (2014) Total antioxidant capacity is significantly lower in cocaine-dependent and methamphetamine-dependent patients relative to normal controls: results from a preliminary study. Hum Psychopharmacol 29:537–543. https://doi.org/10.1002/hup.2430

Zhao Q, Pahlmark K, Smith ML, Siesjo BK (1994) Delayed treatment with the spin trap alpha-phenyl-*n*-*tert*-butyl nitrone (PBN) reduces infarct size following transient middle cerebral-artery occlusion in rats. Acta Physiol Scand 152:349–350. https://doi.org/10.1111/j.1748-1716.1994.tb09816.x

Publisher's Note Springer Nature remains neutral with regard to jurisdictional claims in published maps and institutional affiliations.